A Comparison between Class-E DC-DC Design Methodologies for Wireless Power Transfer

Andrea Celentano*, Fabio Pareschi*,¶, Virgilio Valente†, Riccardo Rovatti§,¶, Wouter A. Serdijn‡, Gianluca Setti*,¶
* DET – Politecnico of Torino, Corso Duca degli Abruzzi 24, 10129 Torino, Italy.
email:{andrea.celentano, fabio.pareschi, gianluca.setti}@polito.it
† Department of Electrical, Computer, and Biomedical Engineering – Ryerson University, Toronto, Canada. email: vvalente@ryerson.ca
‡ Section Bioelectronics – Delft University of Technology, The Netherlands. email: w.a.serdijn@tudelft.nl
§ DEI – University of Bologna, viale Risorgimento 2, 40136 Bologna, Italy. email: riccardo.rovatti@unibo.it
¶ ARCES – University of Bologna, via Toffano 2/2, 40125 Bologna, Italy.

***Abstract*—We consider the design of Wireless Power Transfer (WPT) systems based on inductive links and focus on recent works where the whole WPT system (i.e. both energy transmitter and energy receiver) is designed as an isolated resonant class-E DC-DC converter characterized by a loosely-coupled transformer. The aim of this work is to compare the classic WPT design approach with a novel one, which allows achieving the same performance with a significant reduction in the number of reactive components of the circuit, with beneficial effects in terms of system complexity, size, and cost. We will also show that such a reduction in the number of reactive components leads to improved performance robustness to variations in the inductive link coupling factor.**

I. Introduction

Wireless Power Transfer (WPT) is an emerging technique that aims to replace standard wired power supply in an increasing amount of applications, both industrial and biomedical. Focusing on near field transfer only, two basic WPT methodologies can be identified, namely inductive [1], [2] and capacitive coupling [3], [4]. Based on the magnetic field, the first technique results in fewer adverse effects on the human body with respect to the second one, which is based on the electric field. As a result, inductive coupling is the best choice for WPT biomedical applications. Furthermore, even though circuits based on capacitive coupling can often achieve higher power transfer efficiency than those based on inductive coupling, the performance of the former dramatically drops when the working condition slightly deviates from the nominal one.

We, therefore, focus here on WPT circuits based on inductive coupling and on resonant architectures, that allow higher oscillation frequency and consequently a smaller size of reactive circuit elements. Furthermore, since an inductive link is electrically equivalent to a loosely coupled transformer (i.e., a transformer with a low coupling factor k), we can model WPT systems based on inductive coupling as isolated DC-DC converters (embedding a low-k transformer), where the transmitter and the receiver play the role of the primary and secondary side, respectively. This allows us to exploit all the know-how on the design of isolated converters in the design of inductive coupling WPT systems. The main challenge of this approach is represented by the low coupling factor k, and by its sensitivity on both coils distance and misalignment, which should be carefully checked in any design. The aim of this paper is to investigate the properties of two WPT systems based on two different isolated power converters topologies, and, in particular, their robustness with respect to k.

The design of a resonant isolated DC-DC converter, class-E particularly [5], is not straightforward due to the components non-linearity and the number of reactive elements, which typically makes it impossible to find a closed-form solution able to describe the system evolution. As such, the so called sinusoidal approximation technique is commonly adopted [6], with negative consequences both in terms of exactness of the solution, and of the needs of additional components in the circuit topology to make such an approximation justifiable.

It is also important to stress that a class-E converter is usually designed for a given operating condition, which could be either the one ensuring the nominal or the maximum output power. To cope with changes in the coupling factor, or even with different output power, a control methodology among the many presented in the Literature may be applied [7], [8]. However, since this work aims to compare the intrinsic properties of the circuit topologies either in the case of a classical design approach or in a novel one, we consider any control strategy to be applied to the designed converters out of the scope of our investigation.

This paper is organized as follows. In Section II we briefly introduce the state of the art of WPT systems based on isolated class-E converter design together with its main issues. In Section III two class-E DC-DC converters, designed to fulfill typical specifications of a WPT system, are presented. The first one is based on a classic design approach, whereas the second one has been designed according to a novel methodology. In Section IV the system performance against coupling factor variations of the two systems is analysed and compared. Finally, we draw the conclusions.

II. State of the art

Inductive links are usually designed to operate at high frequency (i.e. in the MHz range) in order to achieve the desired performance with smaller reactive components (particularly with coupled coils of reduced size). Unfortunately, such an increase in the operating frequency results in increasing losses for conventional hard-switching converters, an issue which is addressed relying on circuits typically used in radio-communication systems and based on soft-switching techniques [9].

More specifically, we focus on the class-E topology, characterized by Zero Voltage Switching (ZVS) and Zero Voltage Derivative Switching (ZVDS). Roughly speaking, ZVS consists of reshaping the voltage waveforms across switches (either controlled, like MOS devices, or uncontrolled, such as diodes) to ensure that they naturally reach the zero level immediately before the switch turn-ON time instant. Additionally, if the zero level is reached with a low derivative, the ZVDS is also satisfied. The achievement of both ZVS and ZVDS is usually considered as the optimal class-E operating condition.

The typical design methodology of class-E WPT separately focuses on the transmitter and the received side. The former is usually composed of a typical RF class-E power amplifier, whose only purpose is to drive the primary coil, which is usually designed to achieve the highest possible efficiency. The latter is independently designed as a harvesting block.

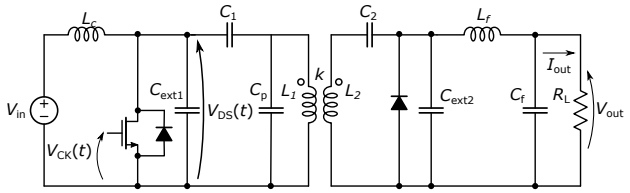

Fig. 1. Schematic of the classic isolated class-E converter (that embeds a low-k transformer) taken from [11].

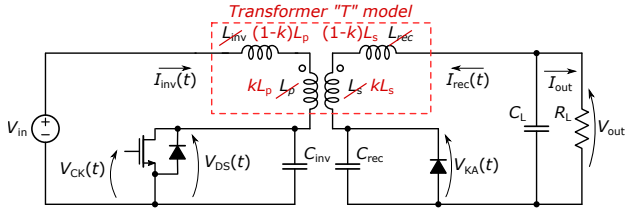

Fig. 2. Schematic of the isolated class-E DC-DC converter (black color) and the modification (red color) derived from the novel approach. The low-k transformer leakage inductances are exploited to avoid extra components.

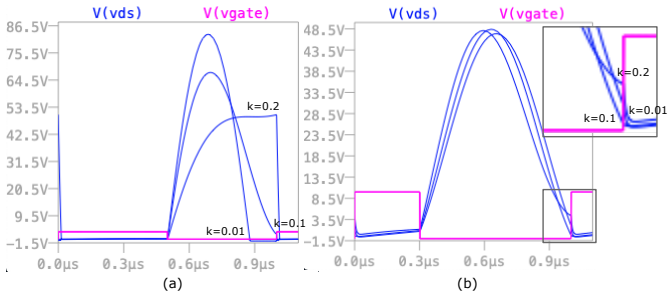

Fig. 3. Spice simulations of the proposed designs showing ZVS or quasi-ZVS for three different values of the coupling factor: $k = 0.01$, $k = 0.1$ and $k = 0.2$. (a): voltage across the MOS with respect to the gate control voltage according to the classical approach. (b): voltage across the MOS with respect to the gate control voltage according to the alternative approach. The top right square box represents a zoom at the clock edge to better distinguish the waveforms.

Only recently, new approaches focusing on the co-design of the transmitter and receiver side have been proposed, which allow considering WPT systems relying on inductive links as loosely coupled isolated DC-DC converters in which the transmitter and the receiver are located at the primary and secondary side, respectively [10], [11]. This results in a more efficient design method than separately considering power amplifier, coils, and rectifier.

Here, we aim to compare two of such design methodologies, applied, respectively, to the circuit schemes shown in Figure 1 and Figure 2, which are analyzed in detail in Section III. The first one is a classic class-E topology, composed by a typical class-E inverter on the left-hand side of the transformer, with the necessary choke inductor and a matching network, and a typical class-E rectifier on the right-hand side, in addition to a second-order filter which is needed before the load. The second one is a much simpler scheme employing the minimum number of components strictly necessary to build an isolated class-E DC-DC converter.

The first and classic approach relies on the so-called sinusoidal approximation, and it is based on the separate design of the inverter stage (providing DC/AC conversion), and of the rectifier one (in charge of AC/DC conversion), and relies on the assumption that the AC component is made of one single harmonic at the switching frequency f_{SW}. Thanks to this, the rectifier circuit can be linearized and averaged and therefore approximated as an equivalent impedance. With this assumption, one can straightforwardly design the class-E inverter as a single-tone power amplifier loaded by the equivalent impedance of the rectifier at the primary side of the transformer. Since the value of such impedance, which also depends on f_{SW} and k, does not usually lead to the optimal class-E inverter load (i.e. the one ensuring that both ZVS and ZVDS holds for the MOS switch) a matching network, designed to work at that particular working point, is added between the main RF power amplifier and the rectifier.

Note that, for the sinusoidal approximation to be effective, additional filtering circuit elements, such as C_1, L_1 and C_2, L_2 tuned on the first harmonic f_{SW} are required. If these elements are not present, the hypothesis grounding the sinusoidal approximation is no longer supported, and this results in appreciable design errors. In the much simpler topology of Figure 2, no circuital elements are introduced to make the sinusoidal approximation reasonable. Therefore, we use the completely different approach proposed in [12], [13] that is based on an exact analysis of the circuit behavior.

III. Class-E Converter Designs

A. Converter specifications

Typical specifications for a loosely coupled class-E DC-DC converter design suitable for a general purpose WPT system are taken from the design example proposed in [11]. The system requires 5 W, with input voltage $V_{in} = 20\,\text{V}$ and $R_{out} = 50\,\Omega$ (so $V_{out} \approx 15.8\,\text{V}$ and $I_{out} \approx 316\,\text{mA}$) operating at the frequency $f_{SW} = 1\,\text{MHz}$. Additionally, the coupled coils result in having a quality factor Q approximately equals to 170 at the nominal frequency and the coupling coefficient is specified to be $k = 0.1$.

B. Classic Class-E Converter Design

In [11], Nagashima *et al.* present a steady state analysis of the isolated class-E converter outside nominal operation. The key point of the analysis is to transform the classic design of a class-E converter, whose schematics is shown in Figure 1, into a typical topology of the class-E inverter: this is somehow equivalent to the classic circuit design methodology previously mentioned.

The class-E inverter is made of a choke inductor L_C, a MOSFET as an active switching device, and three capacitances C_{ext1}, C_1, C_p, which are used to achieve series resonance and impedance transformation. On the other hand, the class-E rectifier consists of a series resonant capacitance C_2, a diode as a non-controlled switching device, an external shunt capacitance C_{ext2}, a second-order low-pass filter $L_f - C_f$ and a load resistance R_L. The two circuits are then connected together by an isolation transformer modeled with two coupled coils L_1 and L_2 with coupling coefficient k.

Regrettably, the major contributions of losses are not taken into account in order not to entangle the analysis. Therefore, the parasitic resistances and the diodes forward voltage drops are assumed to be small enough not to affect the circuit waveforms. As a matter of fact, the dissipated power which occurs in the ESRs, the MOSFET on-resistance and body diode, and diode in the rectifier can only be a-posteriori evaluated. The theoretical analysis, which has also been experimentally validated leads to the following list of components values: $L_1 = 23.1\,\mu\text{H}$, $r_{L_1@1\,\text{MHz}} = 0.891\,\Omega$, $L_2 = 22.7\,\mu\text{H}$, $r_{L_2@1\,\text{MHz}} = 0.829\,\Omega$, $L_C = 284\,\mu\text{H}$, $L_f = 303\,\mu\text{H}$, $C_{\text{ext1}} = 713\,\text{pF}$, $C_1 = 836\,\text{pF}$, $C_p = 434\,\text{pF}$, $C_2 = 1.34\,\text{nF}$, $C_{\text{ext2}} = 2.80\,\text{nF}$, $C_f = 8.35\,\text{nF}$.

The main MOS switch in the design presented in [11] is a SUD06N10-225L from Vishay, switching with a duty cycle $D = 0.5$, and the rectifying diode is a STPS5H100B, a Schottky barrier diode from STMicroelectronics. A screenshot of the drain-source voltage of the MOS switch $V_{DS}(t)$ taken from the Spice simulation is shown in Figure 3(a). From the figure, it can be clearly seen that, for $k = 0.1$, the voltage features quasi-ZVS when the MOS turns on. The slight deviation from the ZVS condition, even for the nominal coupling factor value, is due to the simplifying assumptions on which this classic methodology leans on.

C. Alternative Class-E Converter Design

The simplified circuit of Figure 2 features a simpler architecture by reducing the number of passive components required, as only the coupled coils, two resonant inductors (L_{inv} and L_{rec}) and two resonant capacitors (C_{inv} and C_{rec}) are required. Both L-C filters and the large RF choke inductor have been removed. Due to this, the standard sinusoidal approximation cannot be used for its design. We rely its design on an innovative procedure first proposed in [12] and improved in [13] that is based on the exact analysis of the differential equations regulating the converter evolution, and possibly due to the low number of reactive elements in the circuit. Note that, being this analysis exact, it allows a much more accurate design with respect to the previously considered approximated one. Additionally, this procedure is capable of taking into account the main sources of non-idealities like the losses on the reactive elements, on the MOS switch, and on the rectifier diode.

The low-k transformer embedded in the converter is modeled according to the 'T' model, with a coupling factor k and two inductances L_p and L_s at the primary and secondary side, respectively. As in [14], being the coupling coefficient very low, the two large leakage inductances $(1-k)L_p$ and $(1-k)L_s$ (in red in Figure 2) can be exploited to take the place of the original resonance ones L_{inv} and L_{rec} (in black in Figure 2), while kLp and kLs work as a perfectly coupled transformer. This allows a further reduction in the reactive elements counts, as only the coupled coils and two capacitances C_{inv} and C_{rec} are now required.

Therefore, we configure the transformer to have, for the sake of simplicity, a turn ratio $n_p/n_s = 1$, as well as the transformer of Nagashima *et al.* in [11], and we focus on the solution which allows $L_{inv} = (1-k)L_p$ and $L_{rec} = (1-k)L_s$. While the inductors have been considered to have a quality factor equals to 172, we assume the capacitors to be ceramic with high quality dielectric (e.g., C0G) and therefore with negligible ESR (quality factor $Q > 1000$). For a fair comparison with the classical design approach, which will be carried on in the next section, the main MOS switch is again a SUD06N10-225L (modeled, according to the data-sheet, with an ON resistance $R_{DS}^{ON} = 0.16\,\Omega$ and a forward voltage for the body diode $V_B^{ON} = 0.9\,\mathrm{V}$) and the rectifying diode is a STPS5H100B, (modeled according to the data-sheet with a forward voltage $V_D^{ON} = 0.73\,\mathrm{V}$). The last available degree of freedom for the class-E design is the duty cycle D of the main clock. According to [13] and [15], $D = 30\%$ has been chosen in order to reduce the voltage stress $V_{DS}(t)$ across the main switch. The lower peak value of the $V_{DS}(t)$ can be clearly appreciated in Figure 3. Notice that, if the purpose of the paper had not been the two-methodologies comparison, this would have led to a better choice of the values of the active components, particularly a more suitable MOS transistor, guaranteeing better circuit performance.

By putting the latter data into the model developed in [13], the desired design is achieved for $C_{inv} = 32.9\,\mathrm{nF}$, $C_{rec} = 36.3\,\mathrm{nF}$ and $L_p = L_s = 688.7\,\mathrm{nH}$. A screenshot of the voltage $V_{DS}(t)$, taken from the Spice simulation, is shown in Figure 3(b) where it can be clearly seen that for $k = 0.1$ the voltage exactly reaches the zero voltage level just before the MOS turn-ON instant (ZVS). As described in [13], if k is too low, it is not possible to satisfy both ZVS and ZVDS unless we add an additional inductance. It is worth noting that the beneficial effects deriving from ZVDS are less relevant than the negative consequences deriving from the addition of an extra passive component in terms of power loss, size, and cost.

IV. System performance against coupling factor variations

In a WPT system, the coupling factor, which depends on coils distance, misalignment, and transfer medium, strongly affects the system behavior. Since the design cannot rely on k, these resonant systems must be improved either by modifying the circuit topology or by adding a feedback in a way that they become k-resilient at least in a certain range. In this particular case study, for a fair comparison with [11], no feedback has been considered and the same input/output specifications, as well as the same active devices, have been used. The coupling factor k has been varied from $k = 0.01$ to $k = 0.2$, i.e. from the 10% to the 200% of the nominal value. The consideration of higher k values is not of practical interest in WPT being $k = 0.2$ already difficult to achieve according to [10] and [16].

For $k \neq 0.1$, but in the range $[0.01, 0.2]$, we can say that the system designed according to the alternative methodology, slightly deviates from the sub-optimal condition (ZVS only) and features quasi-ZVS by either reaching an acceptable positive value of $V_{DS}(t)$ at the MOS turn on instant t_{SW}^{ON}, i.e. $V_{DS}(t_{SW}^{ON}) < 4.4\,\mathrm{V}$, or by reaching a negative value greater than the MOSFET body diode forward voltage drop, i.e. $V_{DS}(t_{SW}^{ON}) > -0.9\,\mathrm{V}$. On the other hand, the classical approach just guarantees quasi-ZVS for $k < 0.1$ (either by turning the MOS body diode on or by reaching an acceptable positive $V_{DS}(t_{SW}^{ON})$ value) and heavily deviates from the sub-optimal condition when $k > 0.1$. To this purpose, in Figure 3 the Spice simulations for both design methodologies are depicted in order to show what happens to the voltage across the main switch $V_{DS}(t)$ for the nominal value $k = 0.1$ and for $k = 0.01$ and $k = 0.2$, corresponding to the minimum and maximum coupling factor considered.

The importance of the exact analysis can be appreciated not only because it allows reaching exact ZVS condition, but also because it avoids the use of a matching network, which can provide impedance transformation for just one single specific working point (and so for only one specific k value). Thanks to this, the $V_{DS}(t_{SW}^{ON})$ features k-resilience in a broader coupling factor range by reducing the ZVS condition degradation when the system is designed according to the alternative methodology.

By indicating with the notation $\langle f(t) \rangle$ the average value of $f(t)$ over one period, Figure 4(a), derived from Spice simulations of the circuits of Figure 1 and Figure 2, shows how the efficiency of the two converters η, calculated as $\eta = \langle P_{out} \rangle / \langle P_{in} \rangle$, varies as a function of k. Nagashima *et al.*, as it is shown by the yellow curve of Figure 4(a), obtain an efficiency vs coupling factor curve which has the classical tiny bell shape, which confirms a maximum value $\eta \approx 84\%$ at the nominal coupling coefficient $k = 0.1$ and that quickly decreases as k moves away from the nominal point.

On the other hand, the simplified circuit according to the alternative class-E design features an efficiency $\eta \approx 78\%$ at the nominal coupling factor and it stays above the latter

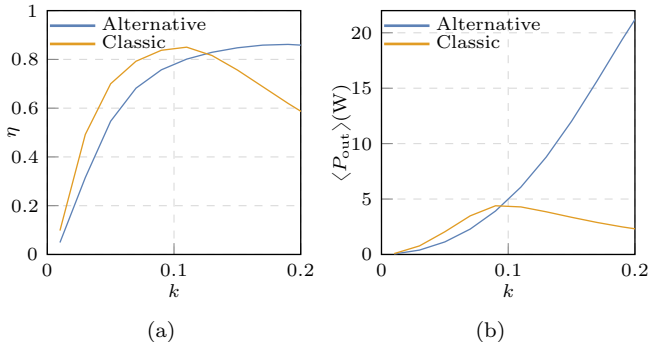

Fig. 4. Comparison of the performances between the two class-E DC-DC converter design methodologies against coupling factor variation. (a): efficiency of the converter calculated as $\langle P_{\text{out}}\rangle/\langle P_{\text{in}}\rangle$; (b): power absorbed by a resistive load $R_L = 50\,\Omega$

value when $k > 0.1$. The efficiency curve of this design is represented by the blue curve in Figure 4(a).

The conclusion which derives from the efficiency analysis is consistent with Figure 3 that shows the higher sensitivity to the coupling factor for the classical design with respect to the alternative one.

Another important difference between the two circuits regards the way the output power $\langle P_{out}\rangle$ changes with the coupling factor. In the simplified topology, as depicted by the blue curve in Figure 4(b) and, contrarily to what happens in the classic design (yellow curve), the power delivered to the load monotonically increases when k increases. Again, since in the classical design methodology the class-E converter is strictly tuned to work just for the designed coupling factor $k = 0.1$, as k changes, the reflected impedance at the primary side is not the optimal one anymore and the power delivered to the secondary side, as well as the one absorbed by the load, decreases. As a matter of fact, the resonance frequency at the primary side deviates from the desired one f_{SW} so that, the ZVS which guarantees the sub-optimal soft-switching condition is lost. The immediate consequence is that the switching power loss at the primary side increases.

Nevertheless, in both cases when k changes, the desired output power $\langle P_{out}\rangle = 5\,\text{W}$ is not guaranteed anymore but, the circuit designed according to the alternative approach is theoretically able to feed the load even for $k > 0.1$.

It is important to point out that the increase of the output power (when the coupling factor increases) can be an enormous advantage in industrial applications such as battery charging or power delivery but, it can be an issue in biomedical applications such as implantable devices, in which the secondary circuit is often located inside the human body and therefore an excess of power can be dangerous (due to the heat generated in the biological tissue). This is one of the reasons why, in conventional class-E solutions, to cope with coupling factor variation, information from the secondary side is needed, which is usually sent back to the transmitter through telemetry. By exploiting the exact design methodology, a very simple technique, which does not need any feedback from the transmitter side has been proved in [10] by making this converter suitable even for biomedical implants. This reduces the complexity of the circuitry, as well as the size and the power overhead, and theoretically let the converter work at the maximum efficiency for any k value.

V. Conclusion

In this paper, two WPT systems based on the design of a low-k class-E isolated DC-DC converter have been considered. In particular, two different design methodologies have been compared: a classical one based on strong simplifying assumptions and a novel one based on an analytical approach recently appeared in the Literature. The performances have been evaluated against coupling factor variations.

The result is a comparable efficiency for the two systems when k is less than the nominal one, whereas the novel approach achieves better performance when k is greater than the nominal one. As a matter of fact, the avoidance of the matching network, as well as the other extra reactive components, has a twofold advantage. Firstly, it results in ZVS satisfaction in a broader k range, and secondly, it allows a significant reduction in the number of reactive components required, affecting the size and cost of the circuit.

The output power study, which has also been investigated, shows that the two circuits behave in a different way making the choice between the two application-dependent.

References

[1] K. van Schuylenbergh and R. Puers, *Inductive Powering: Basic Theory and Application to Biomedical Systems*, ser. Analog Circuits and Signal Processing. Dordrecht: Springer, 2009.

[2] T. Sun, X. Xie, and Z. Wang, *Wireless Power Transfer for Medical Microsystems*. New York: Springer, 2013.

[3] H. Ueda and H. Koizumi, "Class-e2 DC-DC converter with basic class-e inverter and class-e ZCS rectifier for capacitive power transfer," *IEEE Trans. Circuits Syst. II Express Briefs*, vol. 67, no. 5, pp. 941–945, May 2020. doi: 10.1109/TCSII.2020.2981131

[4] E. Abramov, I. Zeltser, M. M. Peretz, and M. M. Peretz, "A Network-Based Approach for Modeling Resonant Capacitive Wireless Power Transfer Systems," *CPSS Transactions on Power Electronics and Applications*, vol. 4, no. 1, pp. 19–29, Mar. 2019. doi: 10.24295/CPSSTPEA.2019.00003

[5] R. Redl, B. Molnar, and N. Sokal, "Class E Resonant Regulated DC/DC Power Converters: Analysis of Operations, and Experimental Results at 1.5 MHz," *IEEE Trans. Power Electron.*, vol. PE-1, no. 2, pp. 111–120, Apr. 1986. doi: 10.1109/TPEL.1986.4766289

[6] M. Kazimierczuk and J. Jozwik, "Resonant DC/DC converter with class-E inverter and class-E rectifier," *IEEE Trans. Ind. Electron*, vol. 36, no. 4, pp. 468–478, Nov. 1989. doi: 10.1109/41.43017

[7] J. M. Burkhart, R. Korsunsky, and D. J. Perreault, "Design Methodology for a Very High Frequency Resonant Boost Converter," *IEEE Trans. Power Electron.*, vol. 28, no. 4, pp. 1929–1937, Apr. 2013. doi: 10.1109/TPEL.2012.2202128

[8] S. Park and J. Rivas-Davila, "Duty cycle and frequency modulations in class-e DC–DC converters for a wide range of input and output voltages," *IEEE Trans. Power Electron.*, vol. 33, no. 12, pp. 10 524–10 538, Dec. 2018. doi: 10.1109/TPEL.2018.2809666

[9] R. Gutmann, "Application of RF Circuit Design Principles to Distributed Power Converters," *IEEE Trans. Ind. Electron. and Control Instr.*, vol. IECI-27, no. 3, pp. 156–164, Aug. 1980. doi: 10.1109/TIECI.1980.351669

[10] A. Celentano *et al.*, "A Wireless Power Transfer System for Biomedical Implants based on an isolated Class-E DC-DC Converter with Power Regulation Capability," in *2020 IEEE 63rd International Midwest Symposium on Circuits and Systems (MWSCAS)*. IEEE, Aug. 2020, pp. 190–193. doi: 10.1109/MWSCAS48704.2020.9184689

[11] T. Nagashima *et al.*, "Steady-state analysis of isolated class-e^2 converter outside nominal operation," *IEEE Trans. Ind. Electron*, vol. 64, no. 4, pp. 3227–3238, Apr. 2017. doi: 10.1109/TIE.2016.2631439

[12] N. Bertoni *et al.*, "An Analytical Approach for the Design of Class-E Resonant DC-DC Converters," *IEEE Trans. Power Electron.*, vol. 31, no. 11, pp. 7701–7713, Nov. 2016. doi: 10.1109/TPEL.2016.2535387

[13] A. Celentano, F. Pareschi, V. R. Gozalez-Diaz, R. Rovatti, and G. Setti, "A Methodology for Practical Design and Optimization of Class-E DC-DC Resonant Converters," *IEEE Access*, pp. 1–1, 2020. doi: 10.1109/ACCESS.2020.3035507

[14] F. Pareschi, A. Celentano, M. Mangia, R. Rovatti, and G. Setti, "Through-The-Barrier Communications in Isolated Class-E Converters Embedding a Low-K Transformer," in *2020 IEEE International Symposium on Circuits and Systems (ISCAS)*, Oct. 2020, pp. 1–5. doi: 10.1109/ISCAS45731.2020.9180486

[15] J. Rivas, O. Leitermann, Y. Han, and D. Perreault, "A very high frequency DC-DC converter based on a class Φ_2 resonant inverter," *IEEE Trans. Power Electron.*, vol. 26, no. 10, pp. 2980–2992, Oct. 2011. doi: 10.1109/TPEL.2011.2108669

[16] M. Schormans, V. Valente, and A. Demosthenous, "Practical Inductive Link Design for Biomedical Wireless Power Transfer: A Tutorial," *IEEE Transactions on Biomedical Circuits and Systems*, vol. 12, no. 5, pp. 1112–1130, Oct. 2018. doi: 10.1109/TBCAS.2018.2846020